Catalyzed β scission of a carbenium ion II — Variations leading to a general mechanism

Qingbin Li and Allan L.L. East

Abstract: The β-scission mechanisms of catalytically chemisorbed carbenium ions are further investigated using density functional theory computations and explicit-contact modelling, but with slightly larger catalyst fragment models than in our previous work. Some variations are seen, including the existence of formal one-step and three-step (rather than two-step) mechanisms. The activation barriers are most affected by the basicity of the catalyst model than by any other characteristics: the stronger the base, the greater the barrier. A general mechanism for β scission is presented, as are the specific mechanisms for all the step variations observed from computations to date.

Key words: C–C bond fission, β scission, carbenium ion, catalysis, chloroaluminate, mechanism.

Résumé : Faisant encore appel à des calculs de théorie de la densité fonctionnelle, on a étudié à nouveau les mécanismes de scission-β d'ions carbénium catalytiquement chimisorbés en faisant de la modélisation de contact explicite et en examinant des modèles de fragments de catalyseur légèrement supérieurs à ceux examinés antérieurement. On a observé des variations, y compris l'existence des mécanismes formels à une et à trois étapes, plutôt que deux étapes. La basicité du modèle du catalyseur est le facteur qui affecte le plus les paramètres d'activation; plus la base est forte, plus grande est la barrière. On présente un mécanisme général pour les scissions β ainsi que des mécanismes spécifiques pour toutes les variétés d'étapes qui ont été observées jusqu'à maintenant à partir des calculs.

Mots clés : scission d'une liaison C–C, scission β, ion carbénium, catalyse, chloroaluminate, mécanisme.

[Traduit par la Rédaction]

Introduction

Catalyzed β scission of the secondary carbenium ion *s*-$C_5H_{11}^+$ on small aluminum-containing anions ($AlH_2(OH)_2^-$ and $AlHCl_3^-$) has been computationally studied by us recently (1). That study filled the holes left by earlier studies of aluminum oxide catalysis of β scission (2–4) and demonstrates qualitative differences in the mechanism due to the different strengths of basicity of the two anions. We have also published β-scission steps found for the larger *s*-$C_6H_{13}^+$ ion on $AlHCl_3^-$ (5).

Real catalytic systems involve condensed phases and are much more difficult to model. Two examples of current interest are solid aluminosilicate zeolites and chloroaluminate ionic liquids. To date, calculations using periodic boundary conditions (6) have been forced to use approximate transition-state-finding algorithms (7) and await improvements. Continuum dielectric models have been problematic for proton-transfer phenomena and may be more so for ionic liquids, although new improvements look promising (8–10).

In this current study, we obtained more B3LYP computational results of minimum-energy pathways for β scission of secondary carbenium ions, initially chemisorbed to various anions. Five systems were studied, $C_5H_{11}^+$ on $Al(OH)(OSiH_3)_3^-$, $C_5H_{11}^+$ on $Al_2Cl_7^-$, $C_6H_{13}^+$ on $Al_2Cl_7^-$, $C_6H_{13}^+$ with a two-fragment catalyst model $AlCl_4^-$ + $AlHCl_3^-$, and $C_6H_{13}^+$ with a three-fragment catalyst model $AlCl_4^-$ + $AlHCl_3^-$ + Na^+. These systems are still poor mimics of real zeolite or ionic liquid systems. However, that is not the point. First, these systems allow us to explore how transition states and mechanisms may change as the models get larger without having to compromise on the accuracy in energy and transition-state calculations. Second, and most importantly, with these 22 new transition states added to the 12 found in our first paper and the 10 relevant ones from ref. 5, we feel we have enough examples to be able to present a truly proper discussion of the β scission of a secondary carbenium ion.

Received 11 July 2006. Accepted 1 September 2006. Published on the NRC Research Press Web site at http://canjchem.nrc.ca on 31 October 2006.

Q. Li and A.L.L. East.[1] Department of Chemistry and Biochemistry, University of Regina, Regina, SK S4S 0A2, Canada.

[1]Corresponding author (e-mail: Allan.East@uregina.ca).

Methods, models, and terminology

Calculations were performed to locate transition states (and the intermediates that they connect) for the β scission of chemisorbed 2-pentenium and 2-hexenium ions, catalyzed by various catalyst models in explicit contact. All computational methods and procedures are the same as before (1), based on the density functional theory model B3LYP (11, 12) with the 6-31G(d,p) basis set (13) and using the PQS 3.0 (14) and Gaussian 98-03 (13) codes. The energies reported have no ZPVE corrections attached, both for consistency with ref. 1 and to maintain focus on the underlying potential energy surface (PES).

For a more zeolite-like aluminosilicate fragment, the 18-atom cluster $Al(OH)(OSiH_3)_3^-$ containing four tetrahedral atoms (denoted T4 model, T=Si, Al), was employed.

 doi:10.1139/V06-143 © 2006 NRC Canada

Compared with the T1 model $AlH_2(OH)_2^-$ used in our previous study (1), the T4 model can better represent the surface of a zeolite, having three surface oxygen atoms and each of these bonded to a silicon atom to make the electron density near the Al and the basicity of the oxygen atoms more realistic. This T4 model has been used in other quantum chemical studies as a zeolite mimic. For example, Svelle et al. used T4 to investigate methylation of methylbenzenes and alkenes by halomethanes and methanol over acidic zeolites (15, 16) and the dimerization of linear alkenes over acidic zeolites (4). Arstad et al. (17, 18) studied the methylation, ethylation, and iso-propylation of methylbenzenes on T4 zeolites. Moreover, Rozanska et al. (19, 20) showed that the relative order of the activation energies of isomerization and transalkylation reactions of toluene and xylenes is conserved when comparing results obtained from T4 with results from larger models using periodic boundary conditions and plane wave basis sets.

For a chloroaluminate ionic liquid fragment, $Al_2Cl_7^-$ was chosen as a first extension over the previously used $AlHCl_3^-$. This choice was motivated by the work in the Johnson group (21). Using B3LYP/6-31G(d,p), Hunter thoroughly examined ionic liquid ion cluster systems involving $AlCl_3$, pyridine (Pyr), and HCl in various ratios and the resulting energies suggested that $PyrH^+$, $Al_2Cl_7^-$, and $AlCl_4^-$ were the predominant species in these mixtures, with extra HCl units complexed to the anions (22).

Further extension of an ionic liquid model was explored using two- and three-fragment catalysis models. The two-fragment model employed both $AlHCl_3^-$ and $AlCl_4^-$ placed on either side of the hydrocarbon and was first tried in an exploration of intermediates (ref. 5, Fig. 9). Since this model produces an overall –1 charge for the system, a three-fragment overall-neutral model was also tested, simply by adding a Na^+ spectator ion to the model. These models were designed to explore the possibility of a lowering of the β-scission barrier by providing a more flexible product chemisorption site option.

As before, we refer to the conversion from chemisorbed to physisorbed structures as ascension and the opposite as descension. We will use single and double slashes to denote chemisorbed and physisorbed complexes, respectively, (eg. $C_6H_{13}^+/AlHCl_3^-$ vs. $C_6H_{13}^+//AlHCl_3^-$). Our atom-numbering convention will be to count the carbon atoms as C_1, C_2, C_3, C_4, and C_5, or for hexane cracking to C_6, such that the C_2 atom is initially bound to the O_1 or Cl_1 atom of the catalyst in the chemisorbed state. A common abbreviation we use is PCP^+ for protonated dialkylcyclopropane, the prevalent form of a physisorbed or gas-phase secondary carbenium ion.

Results

The Cartesian coordinates of the 22 new transition states are provided as Supplementary Material, for purposes of reproducibility.[2] Specific bond distances are not reported in this paper because the important ones hardly differ from the values reported earlier, found with smaller Al-O and Al-Cl anion models (1). The structural results are presented in this section; the energies are left for the Discussion section.

One-fragment catalyst models $T4^-$ and $Al_2Cl_7^-$

Seven transition states (and the minima they connect) were found for the reaction $C_5H_{11}^+ \rightarrow C_2H_5^+ + C_3H_6$ on the T4 zeolite catalyst fragment $Al(OH)(OSiH_3)_3^-$. Five of the seven steps are qualitatively the same as those observed with the T1 model (ref. 1, Figs. 1, 3, and 5). Images of the two qualitatively new steps appear in Fig. 1. The first one (top row), a physi-to-physi β scission, is in comforting agreement with Svelle et al. (4), who observed it with this T4 model and a smaller (6-31G(d)) basis set. Hence, β scission of chemisorbed $C_5H_{11}^+/T4^-$ first rises to physisorbed $C_5H_{10}//T4$, but then could step to either chemisorbed $C_2H_5^+$ or physisorbed C_2H_4. The second row of Fig. 1 shows an extra descension step for the C_2H_4 product, so that we can consider this physi-to-physi β-scission route as a step in a complete chemi-to-chemi mechanism (see Discussion).

Two transition states were found for the two-step scission of $C_6H_{13}^+$ on $AlCl_4^-$. They are no different qualitatively than the two steps found earlier on $AlHCl_3^-$ (1).

Five transition states were found for the reactions $C_5H_{11}^+ \rightarrow C_2H_5^+ + C_3H_6$ (two) and $C_6H_{13}^+ \rightarrow C_3H_7^+ + C_3H_6$ (three) on the $Al_2Cl_7^-$ fragment. Four are qualitatively the same as the two-step "2Cl" (involving two Cl atoms) pathways observed previously for both these carbenium ions on $AlHCl_3^-$ (1, 5). Images for the qualitatively new step appear in the bottom row of Fig. 1. In this step, a physi-to-chemi β-scission step, the physisorbed ion-pair $C_6H_{13}^+//Al_2Cl_7^-$ intermediate undergoes scission, isomerization (p-$C_3H_7^+$ to s-$C_3H_7^+$), and descension (to a chemisorbed s-$C_3H_7^+$ fragment). These three processes are concerted (all in the one step) but not fully synchronous, as the descension occurs in the later part of the step. A similar-looking transition state exists in the $AlHCl_3^-$ fragment pathway (5), but there the forward direction resulted in a proton transfer to the catalyst (generating $HCl{\cdot}AlHCl_2$) rather than to a neighbouring C atom. This discrepancy in product may be due to catalyst basicity or the orientations chosen. In any event, the higher barrier associated with this step (see Discussion) suggests that this isomerization step during β scission will be rare.

Two-fragment catalyst model $AlHCl_3^-$ + $AlCl_4^-$

Figure 2 shows 3D images of the stationary-point geometries obtained for the β scission $C_6H_{13}^+ \rightarrow C_3H_7^+ + C_3H_6$ catalyzed by separated $AlHCl_3^-$ + $AlCl_4^-$ fragments. This model system has an overall charge of –1.

The top two rows of Fig. 2 show the two-step path, as seen with single-fragment catalysis. Here, $AlHCl_3^-$ was chosen as the chemisorbing fragment with $AlCl_4^-$ acting as a spectator fragment physisorbed near the reaction center.

In the third row, concerted one-step chemi-to-chemi β scission is observed, analogous to a one-step mechanism seen before (ref. 1, Fig. 9). Here in Fig. 2, $AlCl_4$ is the chemisorbing fragment with $AlHCl_3^-$ as the physisorbed spectator ion. The ascension of chemisorbed C2 from Cl1 occurs in concert with the S_N2-like migration of the C4 atom

[2] Supplementary data for this article are available on the journal Web site (http://canjchem.nrc.ca) or may be purchased from the Depository of Unpublished Data, Document Delivery, CISTI, National Research Council Canada, Ottawa, ON K1A 0R6, Canada. DUD 5088.

© 2006 NRC Canada

Fig. 1. B3LYP/6-31G(d,p) stationary points for the three qualitatively new steps observed for carbenium ion scission on single anion fragment models. Top row: physi-to-physi scission of 1-pentene on the T4 zeolite catalyst fragment. Middle row: descension of ethene to a chemisorbed ethenium ion. Bottom row: a one-step scission/isomerization/descension of $C_5H_{11}^+$ to C_3H_6 and a chemisorbed *s*-$C_3H_7^+$ fragment on $Al_2Cl_7^-$.

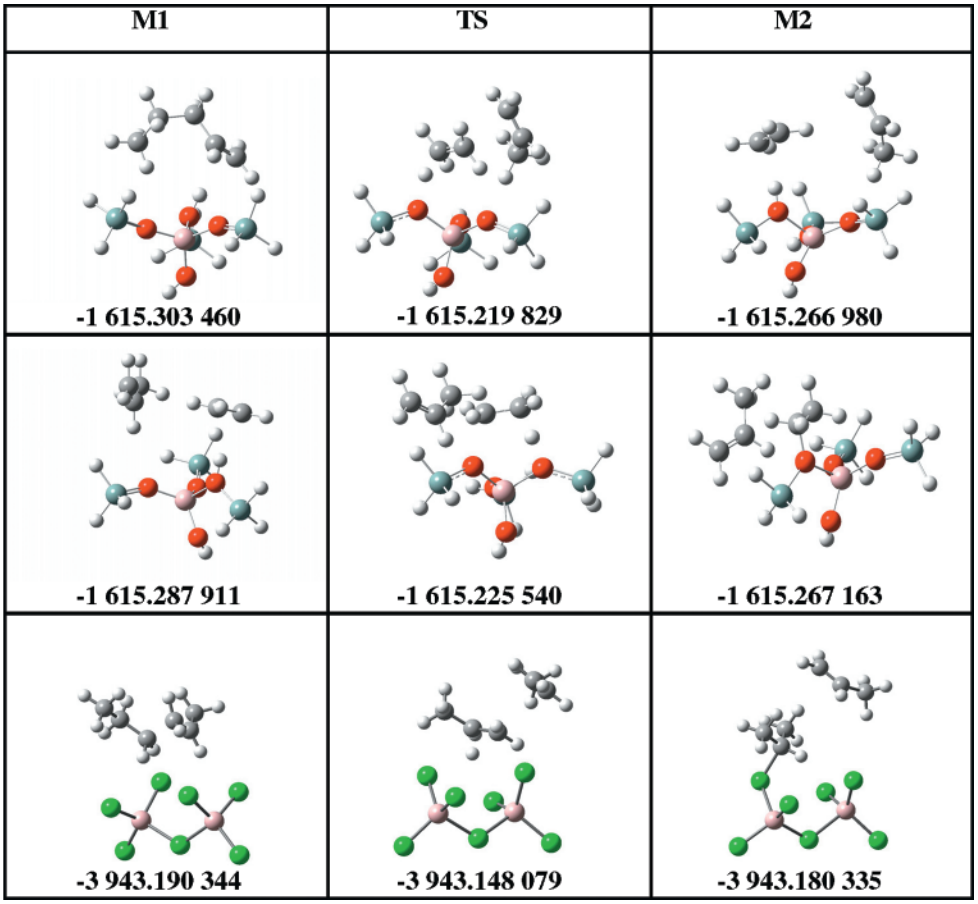

from C3 to Cl2. Subtleties in orientation of the initial structure likely control whether the β scission will be one-step or two-step, since the simpler $AlHCl_3^-$ single-fragment model also exhibited both possibilities (1).

In the last row of Fig. 2, we see another concerted one-step chemi-to-chemi β scission, but here the hydrocarbon migrates from one catalyst fragment ($AlCl_4^-$) to the other ($AlHCl_3^-$). This was the qualitatively new step we hoped to find with the two-fragment catalyst model.

Three-fragment catalyst model $Na^+ + AlHCl_3^- + AlCl_4^-$

Figure 3 shows 3D images of the stationary-point geometries obtained for β scission ($C_6H_{13}^+ \rightarrow C_3H_7^+ + C_3H_6$) in the presence of Na^+ as well as $AlHCl_3^-$ and $AlCl_4^-$ ions. The Na^+ was added to have a neutral charge model system for comparison to the negatively charged model of the previous section. Several choices for the location of the Na^+ ion were tested before settling on one particular choice.

The first two rows show the usual two-step mechanism seen in all chloroaluminate models, here having $AlCl_4^-$ as the chemisorbing fragment and $Na^+ \cdot AlHCl_3^-$ as a spectator complex. The only noteworthy item concerns the first minimum, which shows a peculiar rotation of the tight $Na^+ \cdot AlHCl_3^-$ complex that places the Na^+ near the hydrocarbon.

In the following two rows of Fig. 3, two different one-step chemi-to-chemi β scissions are presented. Unlike the ones in Fig. 2, however, *both* these examples involve a migration from one anion to another, the first from $AlCl_4^-$ to $AlHCl_3^-$ and vice versa for the second. To complicate matters, the addition of Na^+ to the model has created more variety of possible structures, including a saltlike catalyst surface (Fig 3., bottom row). This suggests that the use of three ions in explicit-contact modelling is still a poor model for mimicking liquid-phase transition states.

Discussion

β scission — The general mechanism and its finer details

Our convention considers the reactant and products to be chemisorbed because chemisorbed states are the lower-energy "storage states" of carbenium ions in the presence of oxide and chloride sites. This convention also allows a direct relationship between the reaction activation energy and the strength of the conjugate base of the original Bronsted catalyst (see later).

Given this convention, the general β-scission mechanism is shown in Fig. 4 and consists of three mechanistic components, ascension of the hydrocarbon (A), C–C bond scission

© 2006 NRC Canada

Fig. 2. B3LYP/6-31G(d,p) stationary points for scission of $C_6H_{13}^+$ catalyzed by $AlCl_4^-$ + $AlHCl_3^-$. Top row: ascension from $AlHCl_3^-$. Second row: scission and descension of physisorbed hexenium ion. Third row: one-step scission involving $AlCl_4^-$. Bottom row: one-step scission with migration from $AlCl_4^-$ to $AlHCl_3^-$.

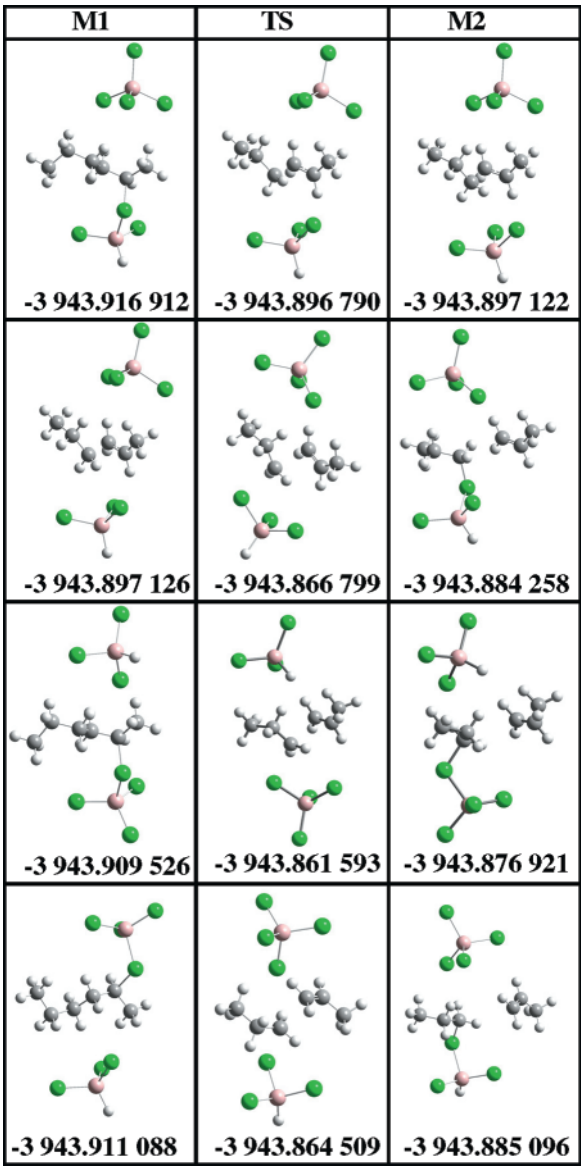

Fig. 3. B3LYP/6-31G(d,p) stationary points for scission of $C_6H_{13}^+$ catalyzed by Na^+ + $AlCl_4^-$ + $AlHCl_3^-$. Top row: ascension from $AlCl_4^-$. Second row: scission and descension of physisorbed hexenium ion. Third row: one-step scission with migration from $AlCl_4^-$ to $AlHCl_3^-$. Bottom row: one-step scission with migration from $AlHCl_3^-$ to $AlCl_4^-$ along a saltlike surface.

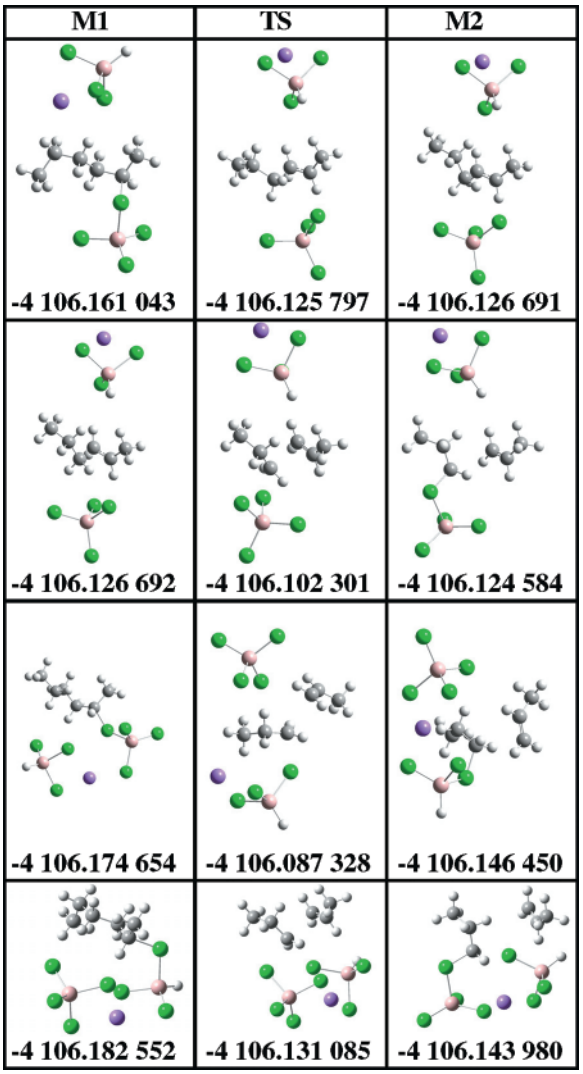

(B), and descension of the resulting primary carbenium ion product (C). In paper I (1), we found the mechanism to be two-step, with ascension to a higher-energy intermediate occurring as a separate step, followed by a concerted scission and descension step. From the work in this paper, we discover that the mechanism could also be one-step or even three-step, depending on catalyst and conformer orientation. Hence, we use the labels "ABC", "A,BC", and "A,B,C" to denote one-step, two-step, and three-step mechanisms.

In addition, Paper I showed that there is some variation in the nature of the physisorbed intermediates. We will denote these here with subscripts, 1 for carbenium ions (PCP^+), 2 for alkenes, and 3 for cyclopropanes. Hence, A_1 will denote

Fig. 4. The general β-scission mechanism from chemisorbed reactant to chemisorbed product. The three components of the mechanism we call ascension (A), scission (B), and descension (C). The mechanism could be one-step, two-step, or three-step, depending on the degree of concertedness of these components.

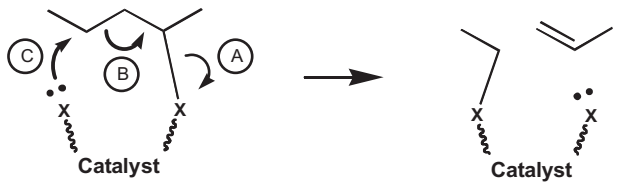

© 2006 NRC Canada

Fig. 5. The various reaction steps seen to date in two-step and three-step β-scission mechanisms from B3LYP calculations using hexenium ion as the example. A, B, C are defined in Fig. 4, while I refers to an isomerization. The subscript labels refer to the type of physisorbed intermediate: 1, carbenium ion (PCP^+); 2, alkene; 3, dialkylcyclopropane.

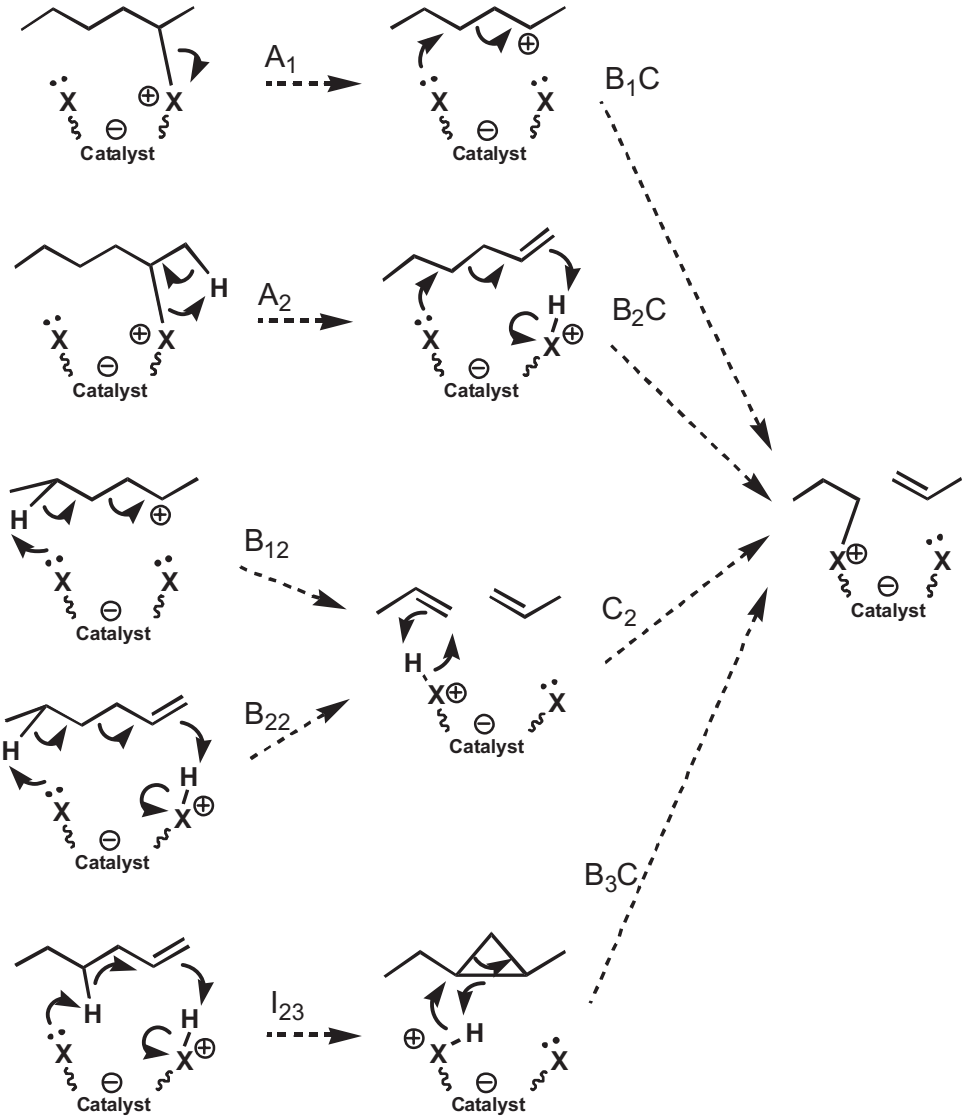

ascension to a physisorbed PCP^+ ion and B_1C will denote concerted scission and descension of this PCP^+ ion. Fig. 5 shows the mechanism for each variation of the steps observed so far.

The B3LYP/6-31G(d,p) relative energies for present and previously published β-scission results are presented in Tables 1 (AlO-containing catalysts) and 2 (AlCl-containing catalysts). Several things are worth commenting on here. First, there is almost no difference in energetics between $C_5H_{11}^+$ and $C_6H_{13}^+$ β scission and there should be no qualitative differences in mechanism either; the A_2 ascensions found with $C_6H_{13}^+/AlHCl_3^-$ also likely exist with $C_5H_{11}^+/AlHCl_3^-$. Second, note the higher energy barriers for both A and BC steps on AlO-containing catalysts vs. AlCl-containing ones. Third, note the qualitative change in intermediates with AlCl-based catalysts; the intermediates can be carbenium ions (note the subscript 1's), unlike the ones with small AlO-based catalysts in which the intermediates are exclusively neutral (subscript 2's and 3's). This was emphasized in paper I and still holds true with the slightly larger catalyst fragments studied here. Fourth, note that the physisorbed carbenium ions of the AlCl-based systems are precariously stable, with barriers of less than 1 kcal mol^{-1} (1 cal = 4.184 J) to returning to the original chemisorbed state.

Single-fragment catalysis

There is a direct relationship between the overall activation barrier for the complete chemi-to-chemi β scission and the strength of the Lewis base sites on the catalyst. A simple indicator of the Lewis base strength of these sites is their proton affinity (PA): the higher the PA, the more basic the nucleophilic site must be. In our tables, we call this calculated PA the conjugate-base proton affinity (CBPA) to remind the reader that the original catalyst for C–C bond cracking is assumed to be a Bronsted acid that has been de-

© 2006 NRC Canada

Table 1. Relative and activation energies (E and E_a, in kcal mol^{-1}) for β-scission steps on AlO-containing catalysts.

Step label	Step	E (M1)	E (TS)	E (M2)	E_a
$C_5H_{11}^+$ on $AlH_2(OH)_2^-$ (CBPA = 338), ref. 1					
A_2	Ascension (1O path)	0.00	46.46	12.76	46.46
A_2	Ascension (2O path)	2.13	36.76	13.07	34.63
I_{23}	Pentene to dialkylcyclopropane	12.93	51.75	19.54	38.81
B_3C	Scission of dialkylcyclopropane	19.75	66.57	21.56	46.82
B_2C	Scission of pentene	12.61	66.75	21.34	54.15
$C_5H_{11}^+$ on $Al(OH)(OSiH_3)_3^-$ (CBPA = 311), this work					
A_2	Ascension (1O path)	0.00	41.70	10.53	41.70
A_2	Ascension (2O path)	0.93	34.22	10.66	33.29
I_{23}	Pentene to dialkylcyclopropane	10.67	44.15	17.56	33.47
B_3C	Scission of dialkylcyclopropane	17.57	60.00	21.01	42.43
B_2C	Scission of pentene	10.73	58.51	20.71	47.78
B_{22}	ph–ph Scission[a]	11.18	63.70	34.08	52.52
C_2	Descension of product[a]	33.97	60.11	20.94	26.14

Note: M1 = first minimum, TS = transition state, M2 = second minimum, and CBPA = conjugate-base proton affinity of the catalyst in kcal mol^{-1}, a measure of base strength (calcd. using B3LYP/6-31(d,p)).

[a]Structural images of these steps are presented in Fig. 1.

activated to its conjugate-base anion form before the β-scission reaction occurs. This consideration is not a moot one because these conjugate-base "catalyst fragments" actually inhibit, rather than accelerate, the β-scission reaction: the more basic the fragment, the more energy is required to rise from the chemisorbed state to the rate-determining transition state (which, in all cases, is an ion-pair complex). This apparent anomaly arises only when considering the β-scission reaction alone, for when the complete cracking of a neutral hydrocarbon is considered, these bigger barriers seen with stronger conjugate bases are actually bigger barriers in overall reactions with weaker acids.

Table 3 summarizes the overall ΔE and E_a values for complete chemi-to-chemi β scission on single-fragment catalysts, together with the CPBA values of the catalysts. The reaction energy is 20–22 kcal mol^{-1}, independent of catalyst. However, the activation barriers vary systematically with basicity of the catalyst, roughly following the linear relation E_a = CBPA/2 – 100. Curiously, an equally simple relation between the base strength and the E_a for simple ascension could not be found.

Aluminum chloride catalysis — Multiple-fragment models

For the two-fragment $AlHCl_3^-$ + $AlCl_4^-$ model (Table 2, 6th section), the first two rows describe the now familiar two-step β scission involving a single fragment ($AlHCl_3^-$ in this case with $AlCl_4^-$ as a spectator ion). The energies are closer to those of $Al_2Cl_7^-$ catalysis than $AlHCl_3^-$ catalysis. One-step chemi-to-chemi β scission was also found, analogous to the one-step scission on $AlHCl_3^-$ with no spectator anion, but with the two-fragment model the energies are closer to that of the two-step $Al_2Cl_7^-$ catalysis. Both of these two-fragment mechanisms give an overall ΔE of 20.5 kcal mol^{-1}, changing little from single-fragment models. The fourth row is the migratory two-fragment step we desired with ascension from $AlCl_4^-$ and descension of the product $C_3H_7^+$ onto $AlHCl_3^-$. The E_a dropped only from 30 to 29 kcal mol^{-1}, indicating little benefit to a two-fragment process. The noticeable decrease in ΔE, from 20.5 to 16.3 kcal mol^{-1}, is merely due to the change of the chemisorption host from a weaker base ($AlCl_4^-$) to a stronger one ($AlHCl_3^-$).

A further step in mimicking an ionic liquid might be to add a cation, making the entire model neutrally charged as it is in our single-fragment modelling. With Na^+ added to the $AlHCl_3^-$ side of the hydrocarbon, we again found the two-step mechanism (involving chemisorbed structures solely with $AlCl_4^-$). Interestingly, the energies for this (Table 2, 7th section) look more similar to those of $AlCl_4^-$ catalysis than those from two-fragment modelling with Na^+ absent. We tried to find two-fragment paths, but these revealed dramatic effects of the Na^+ ion. Saltlike structures of the inorganic ions were seen to offer 8–13 kcal mol^{-1} energy stabilization for the intermediates M1 and M2, for both one-step chemi-to-chemi paths. Such structures are more like solids than liquids and reveal the difficulties in trying to mimic ionic liquids in this way.

Conclusions

β scission, considered here to start and finish with carbenium ions chemisorbed to a catalyst, involves three fundamental components, which are ascension, bond scission, and descension. The lowest-energy pathways on AlO- and AlCl-containing catalyst fragments, as computed with B3LYP/6-31G(d,p), are generally two-step mechanisms, with ascension to a physisorbed intermediates preceding the concerted scission-plus-descension second step. A nearly linear relationship exists between the overall barrier height and the proton affinity of the anion catalyst fragment (the conjugate-base of the hypothetical original Bronsted-acid catalyst).

The extension of an AlO-containing catalyst model from $AlH_2(OH)_2^-$ to $Al(OH)(OSiH_3)_3^-$ reduces the catalyst basicity

© 2006 NRC Canada

Table 2. Relative and activation energies (E and E_a, in kcal mol^{-1}) for β-scission steps on AlCl-containing catalysts.

Step label	Step	E (M1)	E (TS)	E (M2)	E_a
$C_5H_{11}^+$ on $AlHCl_3^-$ (CBPA = 276), ref. 1					
A_1	Ascension	0.00	25.28	24.34	25.28
B_1C	Scission	24.34	38.43	21.27	14.09
ABC	ch-ch Scission	0.02	39.66	21.56	39.64
$C_6H_{13}^+$ on $AlHCl_3^-$ (CBPA = 276), ref. 5					
A_1	Ascension	0.00	23.93	23.19	23.93
B_1C	Scission	23.19	37.00	20.23	13.81
A_2	Ascension to 2-hexene (1Cl)	–0.45	25.66	15.76	26.11
A_2	Ascension to 2-hexene (2Cl)	–1.34	18.19	14.89	19.54
B_{12}	ph-ph Scission	22.57	44.76	37.35	22.19
$C_6H_{13}^+$ on $AlCl_4^-$ (CBPA = 268), this work					
A_1	Ascension	0.00	22.07	21.54	22.07
B_1C	Scission	21.54	35.99	20.45	14.45
$C_5H_{11}^+$ on $Al_2Cl_7^-$ (CBPA = 259), this work					
A_1	Ascension	0.00	12.11	11.33	12.11
B_1C	Scission	11.32	29.97	22.33	18.65
$C_6H_{13}^+$ on $Al_2Cl_7^-$ (CBPA = 259), this work					
A_1	Ascension	0.00	10.92	10.42	10.92
B_1C	Scission	10.42	28.46	21.31	18.04
$B_1I_{ps}C$	Scission + isomerization[a]	10.66	37.20	16.94	26.54
$C_6H_{13}^+$ on $AlHCl_3^-$ + $AlCl_4^-$, this work, Fig. 2					
A_1	Ascension	0.00	12.64	12.43	12.64
B_1C	Scission	12.43	31.47	20.51	19.05
ABC	ch-ch One fragment scission	4.64	34.74	25.11	30.10
ABC	ch-ch Two fragment scission	3.66	32.91	19.98	29.25
$C_6H_{13}^+$ on Na^+ + $AlHCl_3^-$ + $AlCl_4^-$, this work, Fig. 3					
A_1	Ascension	0.00	22.13	21.57	22.13
B_1C	Scission	21.57	36.89	22.90	15.32
ABC	ch-ch Two fragment scission	–8.55	46.29	9.16	54.84
ABC	ch-ch Salt scission	–13.51	18.81	10.72	32.32

Note: M1 = first minimum, TS = transition state, M2 = second minimum, and CBPA = conjugate-base proton affinity of the catalyst in kcal mol^{-1}, a measure of base strength (calcd. using B3LYP/6-31(d,p)).

[a]Structural images of this step is presented in Fig. 1.

Table 3. Overall reaction energies and activation energies for chemi-to-chemi β scission (ΔE and E_a, in kcal mol^{-1}) on single-fragment AlO- and AlCl-containing catalyst anion fragments.

Catalyst	Mechanism	CBPA	E_a	ΔE
$AlH_2(OH)_2^-$	A_2,B_2C	338	67	21
$Al(OH)(OSiH_3)_3^-$	A_2,B_2C	311	59	21
$AlHCl_3^-$	A_1,B_1C	276	37–38	20–21
$AlCl_4^-$	A_1,B_1C	268	36	20
$Al_2Cl_7^-$	A_1,B_1C	259	28–30	21–22

Note: For each catalyst, the lowest-energy pathway to lowest-energy products is considered. CBPA = conjugate-base proton affinity of the catalyst in kcal mol^{-1}, a measure of base strength (calcd. using B3LYP/6-31(d,p)).

but not enough to change qualitative aspects of the reaction. The physisorbed intermediates are neutral-pair complexes of either alkene or disubstituted cyclopropane with catalyst, with two-step or three-step mechanisms observed to date. The overall barrier for β scission from the chemisorbed state is lowered from 67 to 59 by using the larger and less basic anion model.

Chloroaluminate catalysis of the β-scission reaction is also hardly changed qualitatively with moderate extension of the models. The physisorbed intermediates that lead to C–C scission are ion-pair $PCP^+//Al_xCl_y^-$ complexes present with each catalyst model, which are always bound by less than 1 kcal mol^{-1} relative to descension to a chemisorbed state. Hence, the formally two-step A_1,B_1C mechanisms might kinetically appear little different from the one-step chemi-to-chemi β-scission paths, which have been found in both

© 2006 NRC Canada

single-fragment and multiple-fragment modelling. Finally, a truly liquid state proved difficult to mimic with multiple ions, which tended to form saltlike (crystalline) complexes on one side of the hydrocarbon.

Acknowledgments

This research was funded by Natural Sciences and Engineering Research Council of Canada (NSERC) and the Canada Foundation for Innovation (CFI). The Laboratory of Computational Discovery (University of Regina) is thanked for computational resources.

References

1. Q. Li and A.L.L. East. Can. J. Chem. **83**, 1146 (2005).
2. M.V. Frash, V.B. Kazansky, A.M. Rigby, and R.A. van Santen. J. Phys. Chem. B, **102**, 2232 (1998).
3. P.J. Hay, A. Redondo, and Y. Guo. Catal. Today, **50**, 517 (1999).
4. S. Svelle, S. Kolboe, and O. Swang. J. Phys. Chem. B, **108**, 2953 (2004).
5. Q. Li, K.C. Hunter, and A.L.L. East. J. Phys. Chem. A, **109**, 6223 (2005).
6. T. Demuth, X. Rozanska, L. Benco, J. Hafner, R. A. van Santen, and H. Toulhoat. J. Catal. **214**, 68 (2003).
7. G. Mills, H. Jonsson, and G.K. Schenter. Surf. Sci. **324**, 305 (1995).
8. C. Lim, D. Bashford, and M. Karplus. J. Phys. Chem. **95**, 5610 (1991).
9. C.P. Kelly, C.J. Cramer, and D.G. Truhlar. J. Phys. Chem. A, **110**, 2493 (2006).
10. M. Namazian, F. Kalantary-Fotooh, M.R. Noorbala, D.J. Searles, and M.L. Coote. THEOCHEM. **758**, 275 (2006).
11. A.D. Becke. J. Chem. Phys. **98**, 5648 (1993).
12. C. Lee, W. Yang, and R.G. Parr. Phys. Rev. B, **37**, 785 (1988).
13. M.J. Frisch, G.W. Trucks, H.B. Schlegel, G.E. Scuseria, M.A. Robb, J.R. Cheeseman, V.G. Zakrzewski, J.A. Montgomery, R.E. Stratmann, J.C. Burant, S. Dapprich, J.M. Millam, A.D. Daniels, K.N. Kudin, M.C. Strain, O. Farkas, J. Tomasi, V. Barone, M. Cossi, R. Cammi, B. Mennucci, C. Pomelli, C. Adamo, S. Clifford, J. Ochterski, G.A. Petersson, P.Y. Ayala, Q. Cui, K. Morokuma, D.K. Malick, A.D. Rabuck, K. Raghavachari, J.B. Foresman, J. Cioslowski, J.V. Ortiz, B.B. Stefanov, G. Liu, A. Liashenko, P. Piskorz, I. Komaromi, R. Gomperts, R.L. Martin, D.J. Fox, T. Keith, M.A. Al-Laham, C.Y. Peng, A. Nanayakkara, C. Gonzalez, M. Challacombe, P.M.W. Gill, B.G. Johnson, W. Chen, M.W. Wong, J.L. Andres, M. Head-Gordon, E.S. Replogle, and J.A. Pople. Gaussian 98. Rev. A.9 [computer program]. Gaussian Inc., Pittsburgh, Penn. 1998.
14. PQS 3.0 [computer program]. Parallel Quantum Solutions, Fayetteville, Ark. 2004.
15. S. Svelle, S. Kolboe, U. Olsbye, and O. Swang. J. Phys. Chem. B, **107**, 5251 (2003).
16. S. Svelle, B. Arstad, S. Kolboe, and O. Swang. J. Phys. Chem. B, **107**, 9281 (2003).
17. B. Arstad, S. Kolboe, and O. Swang. J. Phys. Chem. B, **106**, 12722 (2002).
18. B. Arstad, S. Kolboe, and O. Swang. J. Phys. Chem. B, **108**, 2300 (2004).
19. X. Rozanska, X. Saintigny, R.A. van Santen, and F. Hutschka. J. Catal. **202**, 141 (2001).
20. X. Rozanska, R.A. van Santen, F. Hutschka, and J. Hafner. J. Am. Chem. Soc. **123**, 7655 (2001).
21. J.L. Campbell and K.E. Johnson. J. Am. Chem. Soc. **117**, 7791 (1995).
22. K.C. Hunter. M. Sc. Thesis, University of Regina, Regina, Sask. 2002.

© 2006 NRC Canada